Polymer Chemistry

ROYAL SOCIETY OF CHEMISTRY

PAPER

View Article Online
View Journal | View Issue

Cite this: *Polym. Chem.*, 2025, **16**, 1383

Triblock architecture and PEG hydrophilic blocks enable efficient thermogelation of poly(2-phenyl-2-oxazine)-based worm-gels†

Anna-Lena Ziegler, Andrew Kerr, Florian T. Kaps and Robert Luxenhofer *

Previously, the cooling-induced thermogelation of an amphiphilic ABA type triblock copolymer comprising a central poly(2-phenyl-2-oxazine) (pPheOzi) block flanked by hydrophilic poly(2-methyl-2-oxazoline) (pMeOx) blocks was reported. This process is based on an unusual, cooling-induced transition in polymer self-assembly from spherical to worm-like micelles, for which the PheOzi units are decisive. Here, we investigate this phenomenon further by introducing new variants of amphiphilic pPheOzi-based copolymers to explore the variability of the system. Changing the arrangement of the MeOx and PheOzi constitutional repeat units enables investigation of the influence of the polymer architecture on the thermogelation. We found that a triblock architecture is superior to diblock, gradient and star-like polymer architectures in terms of efficient order–order transition-based thermogelation. In addition, a coupling procedure based on copper-catalyzed azide–alkyne cycloaddition is presented that allows for a direct comparison of pMeOx and PEG as hydrophilic blocks in pPheOzi-based triblocks. Interestingly, PEG hydrophilic blocks also enable rapid worm-formation and show faster gelation as well as increased gel strength. Altogether, our findings provide basic design criteria for improved (pPheOzi-based) worm-gels. The introduced small library of pPheOzi-based copolymer variants can be used for further fundamental studies regarding thermo-responsive transitions in polymer self-assembly.

Received 25th November 2024,
Accepted 6th February 2025

DOI: 10.1039/d4py01345j

rsc.li/polymers

Introduction

Thermoreversible hydrogels based on amphiphilic block copolymers have been widely investigated in the past.[1–4] Primarily, this research has focused on systems that are liquid at room temperature but gel upon heating close to physiological temperature since this allows application as *in situ* gelling biomaterials.[5–8] In contrast, amphiphilic block copolymer solutions that gel upon cooling have been only rarely described in the literature.[9–12] This may be due to the narrow application window of such polymers, but can arguably also be attributed to the lower prevalence of suitable materials. However, polymer solutions that gel upon cooling might be of interest as rheology modifiers,[10] for temperature-triggered (drug) release,[12] as suspension media for gel-in-gel printing, or for the generation of perfusable channels.[13]

Typically, reversible thermogelling properties of amphiphilic block copolymers are attributed to the use of a temperature-sensitive block, which enables temperature-dependent reversible formation of a micellar network.[1] The nature of the micellar network is contingent upon the nanostructures formed by the underlying amphiphilic block copolymer, which in turn depends on the polymer's composition and structure.[2,14,15] Thus, micellar gel networks of BAB-type block copolymers, where A and B signify hydrophilic and hydrophobic/temperature-sensitive blocks, respectively, are generally achieved by bridging of flower-like micelles.[14,16–18] AB and ABA polymers, in contrast, typically undergo gelation due to the packing of regular spherical micelles, as is the case with Pluronics F127.[14,19,20] This ABA type triblock copolymer is arguably the most widely used block copolymer with thermogelling properties in the biomedical field.[21–24] Being composed of hydrophilic polyethylene glycol (PEG) outer blocks and a thermosensitive polypropylene glycol (PPG) central block, it belongs to the class of Pluronic amphiphiles, also known as poloxamers. While most of the Pluronic members do not exhibit reversible thermogelling properties, they do show amphiphilic behaviour, *i.e.*, aggregation in aqueous solutions above the critical micellar temperature and concentration. Interestingly, for some of these amphiphiles, a progressive transition from

Soft Matter Chemistry, Department of Chemistry, Helsinki Institute of Sustainability Science, Faculty of Science, University of Helsinki, PB55 Helsinki, Finland.
E-mail: robert.luxenhofer@helsinki.fi

†Electronic supplementary information (ESI) available: SEC traces, NMR data and MALDI data of synthesized polymers. Kinetic investigation of gradient copolymer synthesis. Additional rheology data and TEM images. See DOI: https://doi.org/10.1039/d4py01345j

spherical micelles towards worm-like micelles upon temperature increase has been reported, mostly in the presence of an electrolyte.[25–29] This transition results from an enlargement of the hydrophobic core radius, following the packing parameter criterion first introduced by Israelachvili for conventional surfactants.[30] Of note, the reversible transition in Pluronic self-assembly is characterized by a viscosity increase, which can eventually lead to gel-like properties.[27] However, due to the narrow phase region of worm-like aggregates, which requires maintaining a delicate balance of hydrophilic and hydrophobic volume fractions, reports on the thermogelation based on Pluronic and other amphiphilic block copolymer worms are relatively scarce.

One of the rare example of thermoreversible gelation based on worm-like micelles (worm-gels) is given by a unique class of shape-shifting diblock copolymers introduced by Armes and coworkers.[31] The thermoreversible behaviour of these systems is attributed to the use of weakly hydrophobic polymer blocks based on hydroxylfunctional (meth)acrylates,[32,33] rather than classical thermoresponsive polymer blocks. These mildly hydrophobic blocks are subject to temperature induced subtle alterations in the degree of partial hydration which enable transitions in polymer self-assembly.[31,34] The first introduced system of this class comprised a hydrophilic poly(glycerol monomethacrylate) (pGMA) and a more hydrophobic poly(2-hydroxypropyl methacrylate) (pHPMA) block.[32] The pGMA-*b*-pHPMA diblock copolymer was shown to undergo a reversible transition from spherical to worm-like micelles upon heating above 21 °C, resulting in the formation of a soft free-standing physical hydrogel due to interworm entanglements. Variation of the system using alternative hydrophilic blocks, such as PEG[35] or poly(2-(methacryloyloxy)ethyl phosphorylcholine) (PMPC),[36] resulted in similar behaviour. However, with the focus being on accessible morphologies, detailed systematic studies of the influence of hydrophilic moieties on gel properties have not been performed.

In 2020, the cooling-induced thermogelation of an ABA-type triblock copolymer system comprised of hydrophilic poly(2-methyl-2-oxazoline) (pMeOx) A blocks and a hydrophobic poly (2-phenyl-2-oxazine) (pPheOzi) B block was described.[37] Unexpectedly, the sol–gel transition of this polymer was also found to be accompanied by a transition in polymer self-assembly from spherical to worm-like micelles.[37,38] The resulting gels could be tuned markedly with regard to their stiffness by varying the concentration, allowing for both rather soft materials at a polymer concentration of 5 wt% (storage modulus $G' \approx 100$ Pa) and very stiff hydrogels at 40 wt% ($G' \approx$ 100 kPa). Importantly, replacement of the hydrophobic PheOzi moieties by slightly different aromatic repeating units, namely 2-phenyl-2-oxazoline (PheOx) or 2-benzyl-2-oxazine (BenzOzi), did not yield a similar order–order transition – and hence did not result in thermogelation upon cooling. In contrast, slight variations of the hydrophilic moieties using poly(2-ethyl-2-oxazoline) (pEtOx) or poly(2-methyl-2-oxazine) (pMeOzi) outer blocks still enabled the formation of worm-like aggregates upon cooling, but reduced gel strength and gelation kinetics. Thus, the PheOzi-moieties appear to be the decisive driving force for the unusual cooling-induced thermogelation of these ABA-type triblock copolymers. However, the impact of the arrangement of hydrophilic and hydrophobic moieties has yet to be considered in the context of the pPheOzi-based copolymer system.

We previously suggested that the order–order transition of the reported pPheOzi-based triblock copolymers is due to a nonclassical interaction between hydrophilic and hydrophobic polymer blocks.[38] Due to the complex nature of polymers in solution, however, the underlying specific interaction remains to be verified, with consideration being given to the involvement of the amide functionality of the poly(2-oxazoline) (POx) and poly(2-oxazine) (POzi)-based hydrophilic blocks. Varying the hydrophilic blocks to polymers with different chemical moieties responsible for the hydrophilicity could therefore help to improve our understanding of the underlying self-assembly mechanism. In this context, a comparison to PEG is particularly desirable, as the hydrophilic POx and POzi polymers pMeOx, pEtOx and pMeOzi have all been discussed as alternatives to PEG in a variety of applications.[39–41] However, PEG/pPheOzi-based copolymers are not readily accessible due to their different polymerization mechanisms.

Here, we introduce new variants of the previously studied pPheOzi-based copolymer system. Altering the arrangement of MeOx- and PheOzi repeat units enables to investigate the influence of the copolymer architecture (triblock, diblock, gradient, star-like) on the cooling-induced thermogelation. In addition, we introduce a polymer coupling procedure based on copper-catalyzed azide–alkyne cycloadditon (CuAAC) which allows for a direct comparison of pMeOx and PEG as hydrophilic blocks in pPheOzi-based triblock copolymers. Unexpectedly, rheological evaluation of the resulting polymers reveals superior performance of PEG hydrophilic blocks with respect to gelation kinetics and gel strength.

Results and discussion

Copolymer synthesis

Synthesis of MeOx/PheOzi-based copolymers with varying architecture (Fig. 1A) was performed by cationic ring-opening polymerization (CROP) of MeOx and PheOzi. While triblock and diblock architectures (pMeOx-*b*-pPheOzi-*b*-pMeOx, **P_T**, and pPheOzi-*b*-pMeOx, **P_D**) were realized by sequential monomer addition, a gradient microstructure (pMeOx-*grad*-pPheOzi, **P_G**) was obtained in a one-step procedure by concurrent copolymerization of MeOx and PheOzi (ESI Fig. S1†). It was verified that a gradient copolymer was obtained. A more detailed description of the copolymerization can be found in the ESI (section 2.5.1†). In addition, a star-like pPheOzi/pMeOx block copolymer ((pPheOzi-*b*-pMeOx)$_4$, **P_S**) was prepared using the 4-arm initiator pentaerythritol tetrakistriflate. **P_T**, **P_D** and **P_G** were all designed to have a comparable amphiphilic ratio of 15 hydrophobic PheOzi to 70 hydrophilic MeOx units. For **P_S**, in turn, a degree of polymerization of 7.5

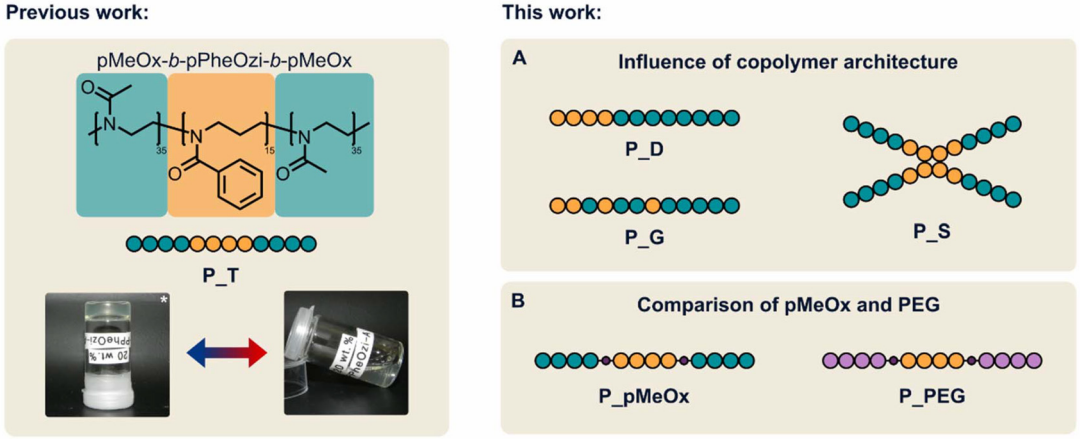

Fig. 1 Overview of the new pPheOzi-based copolymer variants. (A) Schematic representation of a diblock (**P_D**), gradient (**P_G**) and starlike copolymer (**P_S**) structure based on pMeOx and pPheOzi as variants of the previous reported[37] pMeOx/pPheOzi-based triblock copolymer (**P_T**). (B) Schematic representation of pMeOx/pPheOzi and PEG/pPheOzi-based triblock copolymers obtained through a polymer coupling approach (**P_pMeOx** and **P_PEG**) as variants of the previous reported pMeOx/pPheOzi-based triblock copolymer (**P_T**). *Image published previously by Hahn *et al.*[37]

for PheOzi and 35 for MeOx per arm was targeted. Thus, **P_S** can be seen as two linked triblocks with reduced degrees of freedom. Analysis by size exclusion chromatography (SEC) revealed a narrow and essentially monomodal molar mass distribution for all four polymers, indicating successful syntheses (ESI Fig. S2A†). For further details regarding syntheses and characterization, the reader is referred to the ESI (Fig. S2†).

To enable a direct comparison of PEG and pMeOx as hydrophilic corona in the inverse thermogelling pPheOzi-based triblock copolymer system (Fig. 1B), a coupling procedure based on CuAAC was established. Our coupling strategy involved a difunctional alkyne-pPheOzi-alkyne derivative, which was prepared using propargyl tosylate as initiator and potassium pentynoate salt as terminating reagent in the respective CROP (Fig. 2A and ESI Fig. S3†). The successful synthesis of the desired homopolymer structure was evidenced by matrix-assisted laser-desorption–ionization time-of-flight mass spectrometry (MALDI-ToF MS) showing a very narrow molecular weight distribution (Fig. 2B) and the presence of essentially a single distribution of peaks with good agreement of obtained and calculated *m*/*z* values (Fig. 2C). The latter aspect implies that the use of propargyl tosylate and potassium pentynoate in CROP enables high initiation and termination efficiency. Thus, this strategy introduced here could be generally promising to obtain di-alkyne-functionalized POx and POzi derivatives.

With the alkyne units on the pPheOzi homopolymer, an azide end group functionality was required for the hydrophilic polymers pMeOx and PEG. For pMeOx, the azide functionality was realized by terminating the respective CROP with NaN_3 (ESI Fig. S4†).[42] PEG-N_3, in turn, was obtained by quantitatively converting the hydroxyl group of commercially available mPEG-OH into an azide functionality following a literature procedure (ESI Fig. S5†).[43]

In the CuAAC-based polymer coupling procedure (Fig. 3A), we used the azide-containing homopolymer in an excess (1.25 eq. per alkyne moiety) to ensure complete conversion of the pPheOzi alkyne moieties, thus reducing possible diblock copolymer by-product. To remove the remaining excess hydrophilic polymer from the coupling products, we – inspired from protein separation – employed salt-induced precipitation in combination with dialysis as purification method. Here, we utilized the fact that the pPheOzi-based triblock copolymers require lower $(NH_4)_2SO_4$ salt concentration to precipitate in aqueous solution compared to the corresponding hydrophilic homopolymers. Success of this strategy was evidenced by SEC measurements, indicating effective removal of residual hydrophilic homopolymer (Fig. 3B). Finally, to separate any remaining salts, in particular residual copper salts, from the polymer product, we filtered solutions of the coupled triblock copolymers through a plug of $SiO_2/MgSO_4$ (Fig. 3C). This method has previously proven to be suitable for removing NaN_3 from polymers[43] and here also appears appropriate for removing copper salts. Thus, we obtained well-defined and comparable pMeOx-*b*-pPheOzi-*b*-pMeOx (**P_pMeOx**) and PEG-*b*-pPheOzi-*b*-PEG (**P_PEG**) triblock copolymers with minimal residual copper contents (27 ppm for **P_pMeOx**, 15 ppm for **P_PEG**). Of note, our coupling procedure is not limited to the examples presented here but can be applied to other azide-functionalized hydrophilic polymers. This is currently being utilized in our lab for the preparation of a larger block copolymer library. Detailed description of the polymer coupling and characterization can be found in the ESI (Fig. S6 and S7†).

In summary, this study presents five new variants of the pPheOzi-based polymer system which enable the investigation of the influence of polymer architecture and hydrophilic corona on the thermogelation.

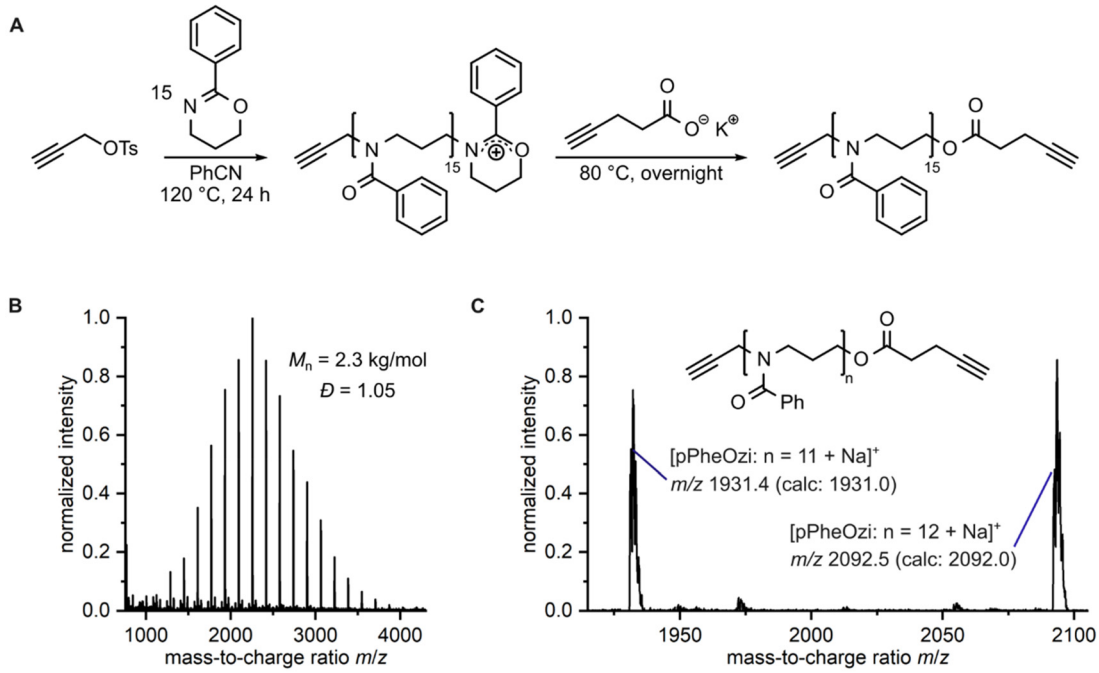

Fig. 2 Successful synthesis of pPheOzi-dialkyne. (A) Synthetic pathway of pPheOzi-dialkyne by CROP of PheOzi using propargyl tosylate as initiator and potassium 4-pentynoate as terminating reagent. (B) MALDI-TOF mass spectrum of the purified pPheOzi-dialkyne recorded in reflector mode. The spectrum was obtained using DCTB as matrix and NaTFA as ionization agent. (C) Spectral expansion of the MALDI-ToF mass spectrum shown in (B) revealing essentially a single species for each DP of pPheOzi-dialkyne that is in accordance with the targeted polymer structure.

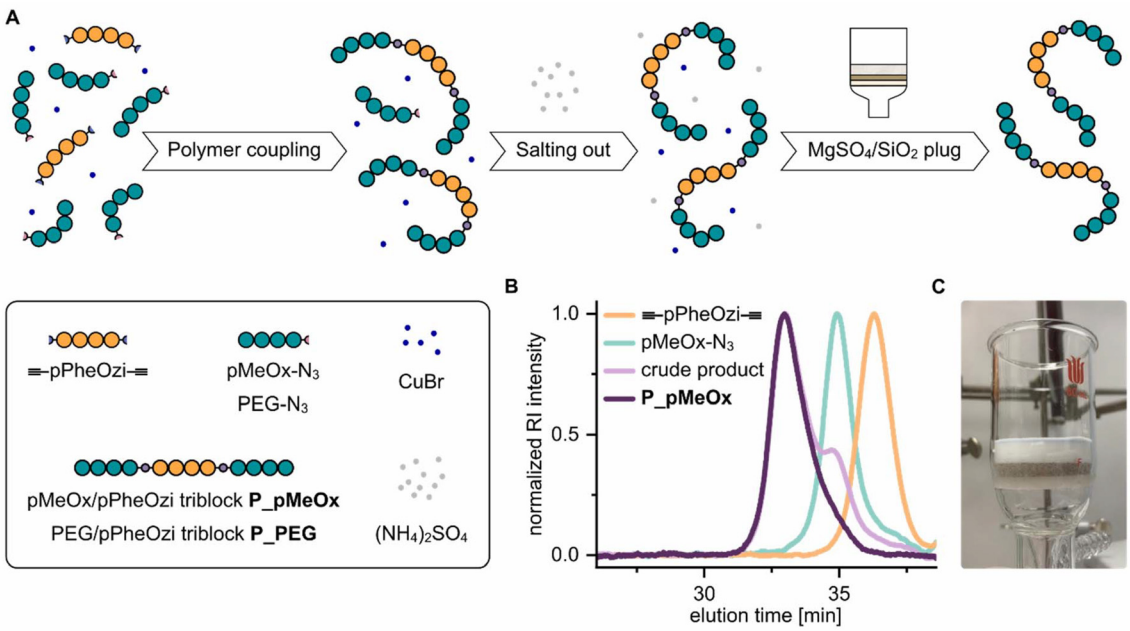

Fig. 3 Coupling protocol for pPheOzi-based ABA triblocks. (A) Schematic representation of the polymer coupling strategy. The coupling reaction involves the pPheOzi dialkyne, an excess of hydrophilic azide-functionalized hydrophilic polymer (pMeOx-N_3 or PEG-N_3, respectively) and the catalyst CuBr. Successfully coupled triblocks are separated from remaining homopolymer by selective precipitation through addition of $(NH_4)_2SO_4$. After dialysis, residual salts are removed by filtration of the polymer through a $MgSO_4/SiO_2$ plug. (B) Size exclusion chromatography elugrams of the P_pMeOx synthesis. Shown are the elugrams of the starting materials pMeOx-N_3 and pPheOzi-dialkyne, the unpurified coupling product containing pMeOx/pPheOzi triblock and pMeOx-N_3 impurity, and the purified product P_pMeOx. (C) $MgSO_4/SiO_2$ plug after filtration of the pMeOx/pPheOzi triblock P_pMeOx showing a fine blue layer on top, indicating separation of copper salts.

Screening for cooling-induced thermogelling behaviour

Self-assembly driven thermogelation is well known to be influenced by polymer composition and architecture.[2] To assess how variations of copolymer architecture and hydrophilic blocks influence the cooling-induced thermogelation of pPheOzi-based systems, we incubated 20 wt% concentrated aqueous solutions of the synthesized copolymers in the fridge for a minimum of 24 hours. Surprisingly, tube-inversion test revealed formation of self-supporting hydrogels for all polymers under investigation (Fig. 4). Gentle heating, in turn, led to liquefaction of the formed gels. Similar to the previously described pPheOzi-based systems, the gelation and liquefaction processes were reversible for all variants introduced here. Of note, the diblock **P_D** and star-like copolymer **P_S** yield markedly more turbid gels compared to the triblock **P_T** and gradient **P_G**. In case of the pMeOx-*b*-pPheOzi-*b*-pMeOx triblock copolymer, weak hydrogels based on a worm network are already formed at low polymer concentrations of 5 wt%.[37] However, reducing the polymer concentration to 5 wt% prevented the gradient and star-like copolymer variants **P_G** and **P_S** from forming self-supporting hydrogels upon cooling, although the viscosity visibly increased. Further experiments addressing the macroscopic gel properties were therefore performed with 20 wt% concentrated aqueous polymer solutions to ensure stable hydrogel formation for all polymers. Of note, the preparation and handling of the samples in the liquid state is straightforward at room temperature due to the long gelation times (ESI Fig. S8A†).

To quantify the gel–sol transition temperature, we performed temperature-dependent rheology measurements (Fig. 4 and ESI Fig. S8B, C†). Similar to previously reported pMeOx-*b*-pPheOzi-*b*-pMeOx triblock copolymer batches,[37,38] **P_T** liquefies at around 30 °C (Fig. 4A). Interestingly, changing the copolymer architecture to a diblock structure has no major influence on the gel–sol transition temperature and gel strength ($G'_{\mathbf{P\_T}} \approx 45$ kPa, $G'_{\mathbf{P\_D}} \approx 34$ kPa, respectively). Compared to **P_T** and **P_D**, the gradient copolymer **P_G** and the star-like copolymer **P_S** show lower persistence against temperature and reduced gel strength ($G'_{\mathbf{P\_G}} \approx 2.2$ kPa and $G'_{\mathbf{P\_S}} \approx 0.3$ kPa, respectively).

The pMeOx-*b*-pPheOzi-*b*-pMeOx triblock **P_pMeOx** displays an almost identical rheological profile compared to **P_T** but exhibits a slightly reduced gel strength ($G'_{\mathbf{P\_pMeOx}} \approx 21$ kPa) (Fig. 4B). It can therefore be assumed that the synthesis protocol (sequential monomer addition *vs.* coupling procedure) does not have a major influence on the reversible thermogelation. Hence, alterations of the rheological profile of **P_PEG** can be attributed to the variation of the hydrophilic blocks and are not primarily a result of the coupling procedure. Interestingly, the 20 wt% **P_PEG** sample displays slightly higher gel strength ($G'_{\mathbf{P\_PEG}} \approx 68$ kPa) and similar gel–sol transition temperature compared to its pMeOx-based counterparts **P_pMeOx** and **P_T**. Previous variations of the pMeOx blocks using EtOx or MeOzi repeat units were shown to reduce both gel strength and the persistence against temperature.[38] The PEG variant is therefore the first alteration of the hydrophilic units of pPheOzi-based triblocks that does not lead to a weakening of the resulting thermogels but shows comparable performance to the "original" pMeOx-*b*-pPheOzi-*b*-pMeOx triblock. In addition, it exhibits a concentration-dependent gel strength (ESI Fig. S8D†), as was previously shown for the pMeOx-*b*-pPheOzi-*b*-pMeOx triblock.[37]

Altogether, our visual and rheological evaluation confirms a high dependency of the thermogel properties on polymer composition and architecture in the case of the pPheOzi-based copolymer system.

New variants form worm-like aggregates upon cooling

Previously, we found that the reversible cooling-induced thermogelation of pMeOx-*b*-pPheOzi-*b*-pMeOx is accompanied by a transition from spherical to worm-like micelles. To investigate whether the thermogelation of the new variants of the

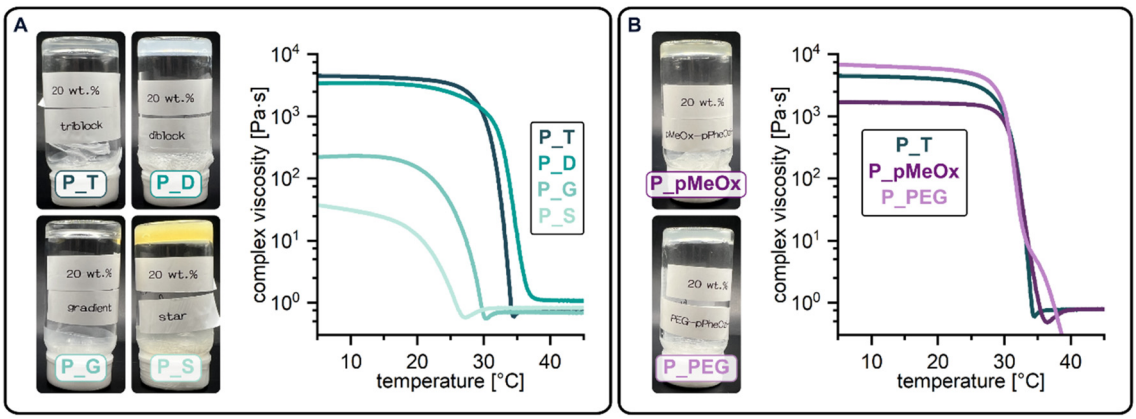

Fig. 4 Screening for the gel–sol transition of pPheOzi-based copolymers. Images show self-supporting gels formed by 20 wt% aqueous solutions of pPheOzi-copolymer variants (A: **P_T**, **P_D**, **P_G** and **P_S**; B: **P_pMeOx** and **P_PEG**) after incubation at 5 °C. Dissolution of the gels is followed by temperature-dependent rheology measurements conducted at 1.0% strain and an angular frequency of 10 rad s^{-1} using an increment rate of 0.5 °C min^{-1}. Liquefaction of the gels is indicated by drastic drop in complex viscosity.

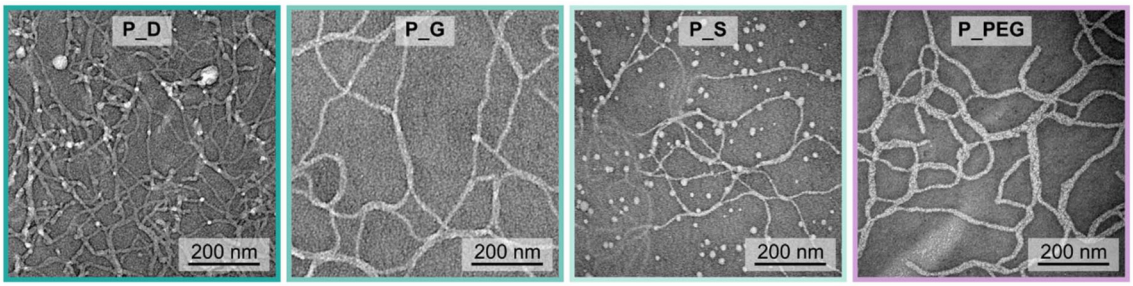

Fig. 5 Presence of worm-like aggregates. Negative stain TEM images obtained of diluted (1 : 125) aqueous polymer solutions (c = 20 g L^{-1}) of **P_D**, **P_G**, **P_S** and **P_PEG** after incubation at 5 °C revealing the presence of worm-like aggregates.

pPheOzi-based system is also linked to the formation of worm-like aggregates, we performed negative stain transmission electron microscopy (TEM) imaging of precooled aqueous polymer solutions (Fig. 5 and ESI Fig. S9†). The obtained images confirm that worm-like aggregates are also formed for all the studied architectures (**P_D**, **P_G** and **P_S**), and when replacing the hydrophilic pMeOx blocks by PEG (**P_PEG**).

Interestingly, while **P_D** and **P_S** seem to form rather thin worm-structures, **P_G** and **P_PEG**-based worm-aggregates appear somewhat thicker and partially also double layered. Further, a notable difference between the samples is the coexistence of spherical aggregates. While spherical aggregates of varying sizes are present in **P_S** images, this is not the case – or at least very much less the case – for the other polymer samples. In addition, partial blurring of the **P_S** worm network is apparent. We interpret this as signs of starting disintegration of the worm-like aggregates, possibly as a result of the sample preparation. Rather unstable worm-aggregates could explain the poor rheological properties of **P_S** and may also result in the rearrangement to spherical aggregates during TEM sample preparation. Thus, at this point it remains unclear whether the occurrence of spherical aggregates in the TEM images of **P_S** is an artefact of the sample preparation or indicates the coexistence of both spherical micelles and worm-like aggregates when equilibrated in the cold.

The confirmation of worm-like aggregates for all pPheOzi-variants indicates that the cooling-induced thermogelation based on a sphere-to-worm transition in polymer self-assembly is not restricted to the triblock pMeOx-*b*-pPheOzi-*b*-pMeOx. Recently, Greenall and Derry used self-consistent field theory to study temperature-dependent transitions in polymer self-assembly.[44] They suggest that a high compatibility between polymer blocks leads to a transition of less curved (worm-like micelles) to more curved suprastructures (spherical micelles) upon increasing the incompatibility of the solvophobic block (here: pPheOzi) and the solvent (here: water). A high compatibility between pMeOx and pPheOzi can be assumed as differential scanning calorimetry (DSC) analysis indicates absence of microphase separation of the blocks in the bulk (ESI Fig. 1C†) and in previous work a nonclassical interaction between the blocks in the cold was suggested based on results from in-depth NMR analysis and MD simulations.[38] POx and POzi generally show improved aqueous solubility in the cold, *ergo* a decreased solubility upon heating. Consequently, the transition from worm-like to spherical micelles could be connected with an increasing incompatibility of pPheOzi and water. However, this interpretation is at odds with results from previous NMR data, showing increasing mobility of the pPheOzi moieties upon heating. Following the suggestions by Greenall and Derry, the presence of worm-like aggregates for the PEG/pPheOzi thermogels suggests that PEG and pPheOzi similarly exhibit high compatibility allowing for pronounced polymer–polymer interactions. However, unravelling the underlying mechanism leading to the worm-formation of **P_PEG** is outside the scope of this study and remains to be investigated.

Overall, TEM images indicate that the cooling-induced order–order transition from spheres to worms is not limited to the triblock copolymer pMeOx-*b*-pPheOzi-*b*-pMeOx but also occurs when the system is changed with respect to its arrangement or its hydrophilic units.

Gelation kinetics is dependent on arrangement and hydrophilic units

The cooling-induced order–order transition-based thermogelation does not occur instantaneously. To follow both the gelation upon cooling and the order–order transition for the different pPheOzi-based copolymer variants, we performed time-dependent rheology measurements at 5 °C and obtained micro DSC (μDSC) thermograms of samples incubated at 2 °C for different lengths of time (0 min–24 hours) (Fig. 6 and ESI Fig. S10†). Of note, the different incubation temperatures were chosen to ensure comparability with previous reports.[37,38] At 20 wt%, the triblock copolymer **P_T** gels within one hour (Fig. 6A). Furthermore, **P_T** displays a most prominent peak at around 32 °C in the μDSC thermograms (Fig. 6B), which coincidences with the gel–sol transition and which we previously assigned to the worm-to-sphere transition. Upon increasing the incubation time at 2 °C, the peak maximum and area increase, indicating progression or maturation of the worm-formation. Compared to **P_T**, the gelation of the diblock **P_D** is delayed (Fig. 6A), as is the evolution of the main peak in the μDSC thermograms (Fig. 6C). Additionally, the maximum of the main peak shifts from 29 °C to 35 °C with

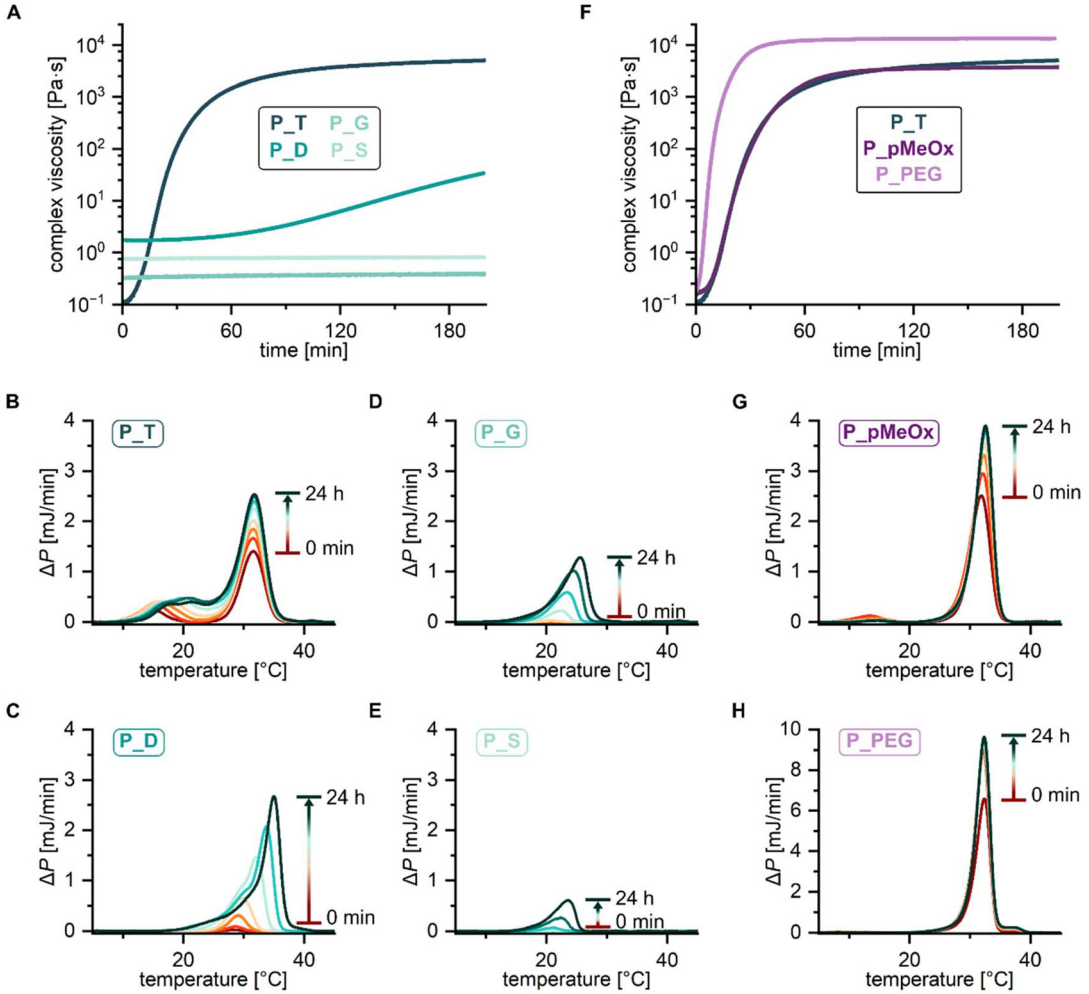

Fig. 6 Kinetics of the sphere-to-worm transition-based thermogelation. A + F Time-dependent rheology measurements of liquid 20 wt% aqueous solutions of **P_T**, **P_D**, **P_G** and **P_S** (A) as well as **P_pMeOx** and **P_PEG** (F) measured at 5 °C, 1.0% strain and an angular frequency of 10 rad s^{-1}. Onset of gelation is indicated by increase in complex viscosity. B–E + G + H μDSC thermograms of aqueous solutions of **P_T** (B), **P_D** (C), **P_G** (D), **P_S** (E), **P_pMeOx** (G) and **P_PEG** (H) incubated at 2 °C in the measurement system for different lengths of time (0 min, 10 min, 30 min, 1 hour, 3 hours, 6 hours, 12 hours, 24 hours).

increasing incubation time at 2 °C. For the gradient and the star-like copolymer, the retardation of the gelling process is even more pronounced (Fig. 6A). Thus, both polymers show no signs of gelation within 3 hours at 5 °C and display a delayed peak evolution in the μDSC thermograms (Fig. 6D and E), *i.e.*, a retarded worm-like aggregate formation. This is consistent with our observation that for **P_G** and **P_S**, the formation of self-supporting hydrogels in the fridge takes the longest time, namely more than 24 hours. In addition, the maximum of the peak in the μDSC thermograms of **P_G** and **P_S** is found below 30 °C, indicating a lower temperature barrier for the dissolution of the worm-like aggregates compared to **P_T** and **P_D**. This is consistent with **P_G** and **P_S** gels also showing lower persistence against temperature. Compared to the triblock, the diblock **P_D** is expected to result in micellar structures with both larger core and shell, thus affecting the resulting packing parameter. This, in turn, seems to impede a fast and efficient sphere-to-worm transition and thus thermogelation. **P_S** was included in this study due to its higher degree of preorganization. In particular, we hypothesized that the worm-formation is facilitated for the star-architecture and may be realized by simple stacking of the polymers. However, our data clearly refute this assumption. This may be due to a more compact core, *i.e.*, micelles with a smaller hydrophobic volume fraction, favouring spherical micelles.

Similar to **P_T**, the coupled pMeOx/pPheOzi-based triblock **P_pMeOx** gels within an hour (Fig. 6F). The agreement of the rheology kinetic measurement curves of **P_T** and **P_pMeOx** corroborates that the thermogelation is largely unaffected by the synthesis protocol, *i.e.*, the triazole linker between the blocks. However, μDSC thermograms indicate the absence of the secondary peak at lower temperature present for **P_T**. So far, we were unable to hypothesize on the molecular origin of this second transition. Hence, at this point it remains unclear

how the additional triazole linkers lead to the diminution of this second peak. Interestingly, for the PEG-based triblock **P_PEG** the gelation is much faster compared to the pMeOx-based counterparts. Incubation at 5 °C leads to an immediate increase in complex viscosity, with the gelation process being completed within 30 minutes. The rapid gelation of **P_PEG** is consistent with the faster attainment of the peak equilibrium in the μDSC thermograms compared to **P_pMeOx** (Fig. 6G and H). This indicates that the hydrophilic PEG blocks enable efficient transition from spherical to worm-like micelles and hence are convenient for the cooling-induced thermogelation.

Altogether, time-dependent rheology measurements and μDSC data suggest that compared to the diblock, gradient and star-like copolymer architecture, the triblock structure has the best combination of packing parameter and macromolecular dynamics to enable efficient rearrangement from spherical to worm-like micelles and thus fast gelation. In addition, PEG-based hydrophilic blocks seem to be favourable for the gelation process.

Conclusions

In this study, we introduced new variants of pPheOzi-based thermogels to address the influence of the polymer architecture and the hydrophilic blocks. Among the polymers with varying arrangement of MeOx and PheOzi repeat units, the triblock structure showed superior performance regarding gel strength and gelation kinetics. This finding can serve as a design criterium for the improvement of other worm-gels. Apparently, the combination of packing parameter and macromolecular dynamics of the triblock architecture is favourable for a fast and efficient sphere-to-worm transition-based thermogelation. In addition, we established a polymer coupling procedure to realize comparable pMeOx/pPheOzi and PEG/pPheOzi triblock copolymers. The replacement of hydrophilic pMeOx blocks by PEG accelerated the gelation process, which makes the system more convenient for applications such as in bioprinting. In addition, the introduction of the PEG/pPheOzi-triblock enables further studies intended to address the unusual transition in self-assembly. In this respect, the different nature of PEG and pPheOzi facilitates the analysis for instance due to clearly distinguishable signals of the blocks in NMR and IR. Beyond that, the introduced coupling procedure is not limited to the two examples presented in this study. Designing triblock copolymers *via* polymer coupling can thus allow to investigate the influence of a variety of hydrophilic blocks, for instance when using block copolymer micelles for drug delivery.

Author contributions

Conceptualization: R. L., A. L. Z.; funding acquisition: R. L.; investigation: A. L. Z., F. T. K.; methodology: A. L. Z., A. K.; resources: R. L.; supervision: R. L.; validation: R. L., A. L. Z.; visualization: A. L. Z.; writing – original draft: A. L. Z.; writing – review & editing: R. L., A. L. Z., F. T. K., A. K.

Data availability

All data presented in this article are available at Zenodo at **https://doi.org/10.5281/zenodo.14215916**.

Conflicts of interest

The authors declare no conflict of interests.

Acknowledgements

This work was supported by the Research Council of Finland (decision number: 342983 awarded to R. L.). A. L. Z. acknowledges financial support through the CHEMS doctoral programme at the University of Helsinki. We gratefully acknowledge support by Sami-Pekka Hirvonen for SEC measurements and Liliia Simagina for NMR kinetic measurements. Furthermore, we thank Electron Microscopy Unit of the Institute of Biotechnology, University of Helsinki, for providing laboratory facilities and acknowledge technical assistance by Mervi Lindman.

References

1 M. T. Cook, P. Haddow, S. B. Kirton and W. J. McAuley, Polymers Exhibiting Lower Critical Solution Temperatures as a Route to Thermoreversible Gelators for Healthcare, *Adv. Funct. Mater.*, 2021, **31** (**8**), 2008123, DOI: **10.1002/adfm.202008123**.

2 A. P. Constantinou and T. K. Georgiou, Tuning the gelation of thermoresponsive gels, *Eur. Polym. J.*, 2016, **78**, 366–375, DOI: **10.1016/j.eurpolymj.2016.02.014**.

3 Q. Lin, C. Owh, J. Y. C. Lim, P. L. Chee, M. P. Y. Yew, E. T. Y. Hor and X. J. Loh, The Thermogel Chronicle–From Rational Design of Thermogelling Copolymers to Advanced Thermogel Applications, *Acc. Mater. Res.*, 2021, **2**(10), 881–894, DOI: **10.1021/accountsmr.1c00128**.

4 T. T. Hoang Thi, L. H. Sinh, D. P. Huynh, D. H. Nguyen and C. Huynh, Self-Assemblable Polymer Smart-Blocks for Temperature-Induced Injectable Hydrogel in Biomedical Applications, *Front. Chem.*, 2020, 8, DOI: **10.3389/fchem.2020.00019**.

5 A. K. Pandya, L. K. Vora, C. Umeyor, D. Surve, A. Patel, S. Biswas, K. Patel and V. B. Patravale, Polymeric in situ forming depots for long-acting drug delivery systems, *Adv. Drug Delivery Rev.*, 2023, **200**, 115003, DOI: **10.1016/j.addr.2023.115003**.

6 T. Li, Q. Bao, J. Shen, R. V. Lalla and D. J. Burgess, Mucoadhesive in situ forming gel for oral mucositis pain

control, *Int. J. Pharm.*, 2020, **580**, 119238, DOI: 10.1016/j.ijpharm.2020.119238.

7 M. Agrawal, S. Saraf, S. Saraf, S. K. Dubey, A. Puri, U. Gupta, P. Kesharwani, V. Ravichandiran, P. Kumar, V. G. M. Naidu, *et al.*, Stimuli-responsive In situ gelling system for nose-to-brain drug delivery, *J. Controlled Release*, 2020, **327**, 235–265, DOI: 10.1016/j.jconrel.2020.07.044.

8 D. Zhao, Y. Rong, D. Li, C. He and X. Chen, Thermo-induced physically crosslinked polypeptide-based block copolymer hydrogels for biomedical applications, *Regener. Biomater.*, 2023, **10**, rbad039, DOI: 10.1093/rb/rbad039.

9 I. A. Parmar, A. S. Shedge, M. V. Badiger, P. P. Wadgaonkar and A. K. Lele, Thermo-reversible sol–gel transition of aqueous solutions of patchy polymers, *RSC Adv.*, 2017, **7**(9), 5101–5110, DOI: 10.1039/C6RA27030A.

10 L. Hahn, E. Karakaya, T. Zorn, B. Sochor, M. Maier, P. Stahlhut, S. Forster, K. Fischer, S. Seiffert, A.-C. Pöppler, *et al.*, An Inverse Thermogelling Bioink Based on an ABA-Type Poly(2-oxazoline) Amphiphile, *Biomacromolecules*, 2021, **22**(7), 3017–3027, DOI: 10.1021/acs.biomac.1c00427.

11 L. Hahn, L. Keßler, L. Polzin, L. Fritze, S. Forster, H. Helten and R. Luxenhofer, ABA Type Amphiphiles with Poly(2-benzhydryl-2-oxazine) Moieties: Synthesis, Characterization and Inverse Thermogelation, *Macromol. Chem. Phys.*, 2021, **222**(17), 2100114, DOI: 10.1002/macp.202100114.

12 H. Zhang, S. Guo, S. Fu and Y. Zhao, A Near-Infrared Light-Responsive Hybrid Hydrogel Based on UCST Triblock Copolymer and Gold Nanorods, *Polymers*, 2017, **9**(6), 238, DOI: 10.3390/polym9060238.

13 J. Kajtez, M. F. Wesseler, M. Birtele, F. R. Khorasgani, D. Rylander Ottosson, A. Heiskanen, T. Kamperman, J. Leijten, A. Martínez-Serrano, N. B. Larsen, *et al.*, Embedded 3D Printing in Self-Healing Annealable Composites for Precise Patterning of Functionally Mature Human Neural Constructs, *Adv. Sci.*, 2022, **9**(25), 2201392, DOI: 10.1002/advs.202201392.

14 K. Zhang, K. Xue and X. J. Loh, Thermo-Responsive Hydrogels: From Recent Progress to Biomedical Applications, *Gels*, 2021, **7**(3), 77, DOI: 10.3390/gels7030077.

15 S. J. Bae, J. M. Suh, Y. S. Sohn, Y. H. Bae, S. W. Kim and B. Jeong, Thermogelling Poly(caprolactone-b-ethylene glycol-b-caprolactone) Aqueous Solutions, *Macromolecules*, 2005, **38**(12), 5260–5265, DOI: 10.1021/ma050489m.

16 B. D. Monnery and R. Hoogenboom, Thermoresponsive hydrogels formed by poly(2-oxazoline) triblock copolymers, *Polym. Chem.*, 2019, **10**(25), 3480–3487, DOI: 10.1039/C9PY00300B.

17 M. A. da Silva, P. Haddow, S. B. Kirton, W. J. McAuley, L. Porcar, C. A. Dreiss and M. T. Cook, Thermoresponsive Triblock-Copolymers of Polyethylene Oxide and Polymethacrylates: Linking Chemistry, Nanoscale Morphology, and Rheological Properties, *Adv. Funct. Mater.*, 2022, **32**(9), 2109010, DOI: 10.1002/adfm.202109010.

18 A. N. Semenov, J. F. Joanny and A. R. Khokhlov, Associating polymers: Equilibrium and linear viscoelasticity, *Macromolecules*, 1995, **28**(4), 1066–1075, DOI: 10.1021/ma00108a038.

19 M. Kell, Structural studies of aqueous solutions of PEO - PPO - PEO triblock copolymers, their micellar aggregates and mesophases; a small-angle neutron scattering study, *J. Phys.: Condens. Matter*, 1996, **8**(25A), A103–A124, DOI: 10.1088/0953-8984/8/25A/008.

20 C. C. Hopkins and J. R. de Bruyn, Gelation and long-time relaxation of aqueous solutions of Pluronic F127, *J. Rheol.*, 2019, **63**(1), 191–201, DOI: 10.1122/1.5054598.

21 R. N. Shamma, R. H. Sayed, H. Madry, N. S. El Sayed and M. Cucchiarini, Triblock Copolymer Bioinks in Hydrogel Three-Dimensional Printing for Regenerative Medicine: A Focus on Pluronic F127, *Tissue Eng., Part B*, 2021, **28**(2), 451–463, DOI: 10.1089/ten.teb.2021.0026.

22 S. Li, C. Yang, J. Li, C. Zhang, L. Zhu, Y. Song, Y. Guo, R. Wang, D. Gan, J. Shi, *et al.*, Progress in Pluronic F127 Derivatives for Application in Wound Healing and Repair, *Int. J. Nanomed.*, 2023, **18**, 4485–4505, DOI: 10.2147/IJN.S418534.

23 P. J. R. Jaquilin, O. S. Oluwafemi, S. Thomas and A. O. Oyedeji, Recent advances in drug delivery nano-carriers incorporated in temperature-sensitive Pluronic F-127-A critical review, *J. Drug Delivery Sci. Technol.*, 2022, **72**, 103390, DOI: 10.1016/j.jddst.2022.103390.

24 A. P. Constantinou and T. K. Georgiou, Pre-clinical and clinical applications of thermoreversible hydrogels in biomedical engineering: a review, *Polym. Int.*, 2021, **70**(10), 1433–1448, DOI: 10.1002/pi.6266.

25 K. Mortensen and J. S. Pedersen, Structural study on the micelle formation of poly(ethylene oxide)-poly(propylene oxide)-poly(ethylene oxide) triblock copolymer in aqueous solution, *Macromolecules*, 1993, **26**(4), 805–812, DOI: 10.1021/ma00056a035.

26 V. K. Aswal, P. S. Goyal, J. Kohlbrecher and P. Bahadur, SANS study of salt induced micellization in PEO–PPO–PEO block copolymers, *Chem. Phys. Lett.*, 2001, **349**(5), 458–462, DOI: 10.1016/S0009-2614(01)01249-0.

27 M. Duval, G. Waton and F. Schosseler, Temperature-Induced Growth of Wormlike Copolymer Micelles, *Langmuir*, 2005, **21**(11), 4904–4911, DOI: 10.1021/la050177c.

28 D. Löf, K. Schillén, W. Loh and G. Olofsson, A Calorimetry and Light Scattering Study of the Formation and Shape Transition of Mixed Micelles of EO20PO68EO20 Triblock Copolymer (P123) and Nonionic Surfactant (C12EO6), *J. Phys. Chem. B*, 2007, **111**(21), 5911–5920, DOI: 10.1021/jp071101n.

29 J. G. Álvarez-Ramírez, V. V. A. Fernández, E. R. Macías, Y. Rharbi, P. Taboada, R. Gámez-Corrales, J. E. Puig and J. F. A. Soltero, Phase behavior of the Pluronic P103/water system in the dilute and semi-dilute regimes, *J. Colloid Interface Sci.*, 2009, **333**(2), 655–662, DOI: 10.1016/j.jcis.2009.01.068.

30 J. N. Israelachvili, D. J. Mitchell and B. W. Ninham, Theory of self-assembly of hydrocarbon amphiphiles into micelles

and bilayers, *J. Chem. Soc., Faraday Trans. 2*, 1976, **72**, 1525–1568, DOI: **10.1039/F29767201525**.

31 S. J. Hunter and S. P. Armes, Shape-Shifting Thermoresponsive Block Copolymer Nano-Objects, *J. Colloid Interface Sci.*, 2023, **634**, 906–920, DOI: **10.1016/j.jcis.2022.12.080**.

32 A. Blanazs, R. Verber, O. O. Mykhaylyk, A. J. Ryan, J. Z. Heath, C. W. I. Douglas and S. P. Armes, Sterilizable Gels from Thermoresponsive Block Copolymer Worms, *J. Am. Chem. Soc.*, 2012, **134**(23), 9741–9748, DOI: **10.1021/ja3024059**.

33 S. J. Hunter, N. J. W. Penfold, E. R. Jones, T. Zinn, O. O. Mykhaylyk and S. P. Armes, Synthesis of Thermoresponsive Diblock Copolymer Nano-Objects via RAFT Aqueous Emulsion Polymerization of Hydroxybutyl Methacrylate, *Macromolecules*, 2022, **55**(8), 3051–3062, DOI: **10.1021/acs.macromol.2c00379**.

34 N. J. Warren and S. P. Armes, Polymerization-Induced Self-Assembly of Block Copolymer Nano-objects via RAFT Aqueous Dispersion Polymerization, *J. Am. Chem. Soc.*, 2014, **136**(29), 10174–10185, DOI: **10.1021/ja502843f**.

35 N. J. Warren, O. O. Mykhaylyk, D. Mahmood, A. J. Ryan and S. P. Armes, RAFT Aqueous Dispersion Polymerization Yields Poly(ethylene glycol)-Based Diblock Copolymer Nano-Objects with Predictable Single Phase Morphologies, *J. Am. Chem. Soc.*, 2014, **136**(3), 1023–1033, DOI: **10.1021/ja410593n**.

36 D. L. Beattie, O. O. Mykhaylyk, A. J. Ryan and S. P. Armes, Rational synthesis of novel biocompatible thermoresponsive block copolymer worm gels, *Soft Matter*, 2021, **17**(22), 5602–5612, DOI: **10.1039/D1SM00460C**.

37 L. Hahn, M. Maier, P. Stahlhut, M. Beudert, V. Flegler, S. Forster, A. Altmann, F. Töppke, K. Fischer, S. Seiffert, *et al.*, Inverse Thermogelation of Aqueous Triblock Copolymer Solutions into Macroporous Shear-Thinning 3D Printable Inks, *ACS Appl. Mater. Interfaces*, 2020, **12**(11), 12445–12456, DOI: **10.1021/acsami.9b21282**.

38 L. Hahn, T. Zorn, J. Kehrein, T. Kielholz, A.-L. Ziegler, S. Forster, B. Sochor, E. S. Lisitsyna, N. A. Durandin, T. Laaksonen, *et al.*, Unraveling an Alternative Mechanism in Polymer Self-Assemblies: An Order–Order Transition with Unusual Molecular Interactions between Hydrophilic and Hydrophobic Polymer Blocks, *ACS Nano*, 2023, **17**(7), 6932–6942, DOI: **10.1021/acsnano.3c00722**.

39 M. Barz, R. Luxenhofer, R. Zentel and M. J. Vicent, Overcoming the PEG-addiction: well-defined alternatives to PEG, from structure–property relationships to better defined therapeutics, *Polym. Chem.*, 2011, **2**(9), 1900–1918, DOI: **10.1039/C0PY00406E**.

40 X. He, T. J. Payne, A. Takanashi, Y. Fang, S. D. Kerai, J. P. Morrow, H. Al-Wassiti, C. W. Pouton and K. Kempe, Tailored Monoacyl Poly(2-oxazoline)- and Poly(2-oxazine)-Lipids as PEG-Lipid Alternatives for Stabilization and Delivery of mRNA-Lipid Nanoparticles, *Biomacromolecules*, 2024, **25**(7), 4591–4603, DOI: **10.1021/acs.biomac.4c00651**.

41 A. J. D. S. Sanchez, D. Loughrey, E. S. Echeverri, S. G. Huayamares, A. Radmand, K. Paunovska, M. Hatit, K. E. Tiegreen, P. J. Santangelo and J. E. Dahlman, Substituting Poly(ethylene glycol) Lipids with Poly(2-ethyl-2-oxazoline) Lipids Improves Lipid Nanoparticle Repeat Dosing, *Adv. Healthcare Mater.*, 2024, **13**(17), 2304033, DOI: **10.1002/adhm.202304033**.

42 G. Volet, T.-X. Lav, J. Babinot and C. Amiel, Click-Chemistry: An Alternative Way to Functionalize Poly(2-methyl-2-oxazoline), *Macromol. Chem. Phys.*, 2011, **212**(2), 118–124, DOI: **10.1002/macp.201000556**.

43 J. E. Semple, B. Sullivan, T. Vojkovsky and K. N. Sill, Synthesis and facile end-group quantification of functionalized PEG azides, *J. Polym. Sci., Part A: Polym. Chem.*, 2016, **54**(18), 2888–2895, DOI: **10.1002/pola.28174**.

44 M. J. Greenall and M. J. Derry, Temperature dependence of micelle shape transitions in copolymer solutions: the role of inter-block incompatibility, *Soft Matter*, 2024, **20**(17), 3628–3634, DOI: **10.1039/D4SM00331D**.

